

Molecular modeling and simulation study revealed impact of IL-2 mutations on interaction with IL-2 receptor

Uzma Nisar¹, Faiza Saleem^{1*}, Munir Ahmad², Hafsa Amjad¹, Hamza Arshad Dar^{3*}

¹ Department of Biotechnology, Lahore College for Women University Lahore, 54590, Punjab, Pakistan.

² School of Biological Sciences, University of the Punjab, Quaid e Azam campus Lahore, 54590, Punjab, Pakistan.

³ Atta-ur-Rahman School of Applied Biosciences (ASAB), National University of Sciences and Technology, Sector H-12 Islamabad 44000, Pakistan.

Corresponding Authors:

Faiza Saleem¹

Department of Biotechnology, Lahore College for Women University Lahore, 54590, Punjab, Pakistan.

Hamza Arshad Dar³

Atta-ur-Rahman School of Applied Biosciences (ASAB), National University of Sciences and Technology, Sector H-12 Islamabad 44000, Pakistan.

Abstract

In clinical settings, high-dose IL-2 can be used due to its anti-cancer properties. However, there are many problems encountered in this therapy such as toxicity and other side effects. To improve IL-2 based immunotherapies, researchers have studied modified forms of IL-2, including single-point variants of IL-2. In this study, we aimed to study the effect of single-point mutations in IL-2 (F42A, Y45A, and E61A) and its interaction with IL-2R α . Structural modeling and molecular dynamics simulation were conducted to obtain stabilized structures of both IL-2 and its single-point variants. IL-2/IL-2 variant structures were subjected to molecular docking and interaction analyses with IL-2R α . Moreover, Gibbs free energy calculations were performed to understand the thermodynamic aspects of interaction. Optimized high-quality structural models of wild-type IL-2 and its three single-point variants (F42A, Y45A, and E61A) were obtained by molecular modeling and simulations. Overall, our results suggest that these single-point mutations in IL-2 not only preserved the conformational compactness of IL-2 but also enhanced its interaction with cognate IL-2 receptor. The obtained results are in conformity with previous studies and may be helpful to guide the designing of novel IL-2 mutants to improve cancer immunotherapy.

Keywords: Human Interleukin-2; Structural modeling; Molecular dynamics; Docking; In-silico interaction

Introduction

Interleukin-2 is a key cytokine involved in major immunological responses inside human body (Bird et al. 2005; Sun et al. 2019). This protein is majorly produced by both cytolytic and helper T-cells after their activation (Carmenate et al. 2013). For proper stimulation and function of IL-2, it needs to bind to IL-2 receptors. The high-affinity IL-2

receptor is comprised of major subunits α , β , and γ . Whereas, the moderate affinity IL-2 receptor is established by the merger of two subunits to form a dimeric receptor (IL-2R $\beta\gamma$) (Abbas et al. 2018). IL-2 is a growth-stimulating cytokine that enhances the survival, accumulation, and differentiation of antigen-specific lymphocytes (Stauber et al. 2006; Hernandez et al. 2022). Due to its pivotal role in driving highly specific innate and adaptive immune responses, IL-2 can promote anti-tumor activities. Especially, a high IL-2 dose is used as a therapy to obtain increased levels of effector natural killer and effector T cells in cancer patients (Lotze et al. 1985; Rosenberg et al. 1987). In 1992, the FDA approved the first immunotherapy drug Aldesleukin (a synthetic IL-2 protein) to treat renal carcinoma; this drug was also used later to treat metastatic melanoma (Rosenberg et al. 1998).

The direct therapeutic application of IL-2 is not feasible due to toxicity, hypoxia, and other factors (Tang and Harding 2019). Moreover, the binding of IL-2 to IL-2 receptor alpha subunit on lung endothelial cells may cause pulmonary edema (Krieg et al. 2010). IL-2R α is especially overexpressed in regulatory T-cells, therefore IL-2 binding to IL-2 receptor may stimulate the enhanced production of these regulatory immune cells. Consequently, IL-2 mediated stimulation of anti-tumor lymphocytes is greatly impacted (Berraondo et al. 2019). So, averting IL-2 binding to IL-2R α is a good option to reduce toxicity in cancer immunotherapy. In contrast, there are other cases such as autoimmune diseases in which the enhanced production of regulatory T-cells is desired (Saadoun et al. 2011; Mizui and Tsokos 2016; He et al. 2020). In such situations, a low dose of IL-2 has been explored to treat autoimmune diseases.

Modified IL-2 forms can overcome the toxicity issues of standalone IL-2 and provide better pharmacokinetics and pharmacodynamics outcomes. One way to accomplish this task is to maintain or enhance the binding of IL-2 to IL-2R $\beta\gamma$ receptor and also prevent/lessen the binding of IL-2 to IL-2R $\alpha\beta\gamma$ receptor. This can be done by site-directed mutagenesis of IL-2 to minimize binding towards the high-affinity IL-2 receptor. Some IL-2 mutations (R38A or F42K) reportedly promoted binding to IL-2R $\beta\gamma$ receptor and decreased affinity towards IL-2R $\alpha\beta\gamma$ receptor (Heaton et al. 1993, 1994). Whereas Y45A, F24A, and L72G mutations stopped the interaction of IL-2 mutant with the CD25 subunit (Klein et al. 2017). Also, it was found that induced mutations in IL-2 can help small molecule inhibitors inhibit the interaction between IL-2 and CD25 (Thanos et al. 2006).

In this study, we used molecular dynamics (MD) simulations to investigate the flexibility and conformation of IL-2. The study also focuses on some IL-2 variants (F42A, Y45A, and E61A) and compares them with wild-type (WT) IL-2 structure. We therefore designed mutant versions of IL-2, by introducing mutations in three specific residues: F42A, Y45A, and E61A. These mutations were chosen based on their position in the protein and have been explored previously (Sun et al. 2019; Beig Parikhani et al. 2022; L Alaofi and others 2022). Also, we aimed to explore the interactions of both wild-type IL-2 and its single-point variants with IL-2R α . We hope this knowledge will allow researchers to design IL-2 mutants that can interact with the IL-2 receptor with moderated affinity without better interaction with the CD25 subunit.

Materials and Methods

IL-2 sequence and structure retrieval

Human IL-2 sequence was obtained in FASTA format was retrieved from NCBI accession number K02056. The corresponding amino acid sequence was obtained by the ExPasy translate tool (Artimo et al. 2012). This amino acid sequence was subjected to PSI-BLAST against human proteins from the Protein Databank to ascertain whether its crystal structure was available or not.

Structural modeling of IL-2/IL-2 variants and optimizations

To obtain optimized structures, some additional steps were needed. First, all co-crystal and water molecules were removed. All the missing internal residues were modeled by the MODELLER built-in tool using default settings within the UCSF Chimera (Pettersen et al. 2004; Webb and Sali 2016). The best model with highest GA341 score and lowest DOPE energy score of -2.36 was selected. For generating variant structures, mutations were introduced by the UCSF chimera swap amino acid command. Next, the structures of wild-type IL-2 and its single-point variants (F42A, Y45A, and E61A) were subjected to classic molecular dynamics (MD) simulation.

MD simulation of IL-2/IL-2 variant structures

The IL-2 structures were stabilized by the Molecular Dynamics (MD) simulation software GROMACS 2020.4 (Lindahl et al. 2020). GROMACS is a popular Linux-based tool extensively used in biomolecular simulations. The baseline force field-compliant topology was maintained by converting the PDB file to a gro file. An OPLS-AA force field was chosen (Kaminski et al. 2001).

A rhombic dodecahedron cubic box was used to confine the protein and water molecules. The protein structure was placed in the cube's middle, 1 nm from the cube's edge. Water with specific gravity spc216 was used for simulating protein structures. It was held in place by a constant force of $1000 \text{ kJ mol}^{-1} \text{ nm}^{-2}$. A tool called genion was utilized to remove the charge from the protein. To maintain an electrochemically neutral environment, positive sodium ions or negative chloride ions were introduced, depending on the total charge accumulated.

The lowest energy structure was produced after energy minimization steps by the steepest descent algorithm. Using NVT ensemble equilibration steps for 1000 ps, the temperature of the protein was stabilized. Then, using an NPT ensemble with nearly identical parameters, the pressure and densities of stabilized IL-2 structures were calculated. This process took 500,000 steps. Next, a 10 ns MD simulation was performed on the equilibrium-stabilized structures. Results were produced in the form of graphs, and predictions for the RMSD of the initial structure and the RMSD of the energy-minimized backbone were made. Utilizing Xmgrace, the graphs of the energy minimization, RMSD, RMSF, Radius of gyration, and SASA were examined (Turner 2005).

IL-2R α structural modeling

The sequence of IL-2R α was retrieved from the UniProt database (Consortium 2019). A PSI-BLAST was performed on it against human proteins from the Protein DataBank resource (Burley et al. 2018). Due to the non-availability of complete structure, structural modeling was performed. To overcome this issues, Phyre2 (Kelley et al. 2015), SWISS-MODEL (Waterhouse et al. 2018), I-TASSER (Zhang 2008), 3Dpro (Cheng et al. 2005), and Robetta server (Baek et al. 2021) were used. All the crude models obtained thereof were subjected to quality assessment by the ERRAT (Colovos and Yeates 1993) and PROCHECK (Laskowski et al. 1993) online tools hosted by the SAVES server version 6.0. The top-quality structure was then refined by the GalaxyRefine (Heo et al. 2013) web service. Finally, the best model of IL-2R α was identified as per stereochemical and Ramachandran plot analysis. The near-nativeness of this structure was also verified by the ProSA-web server (Wiederstein and Sippl 2007).

Molecular docking and interaction analyses

Molecular docking technique was employed to study the possible interaction mode and binding poses of WT IL-2 and IL-2 variants (F42A, Y45A, and E61A) with IL-2R α . For the IL-2 and its single-point variants, the last MD frame was selected as the optimal and stabilized structure. In order to collect information about potential active site and surrounding residues, the default settings of CPORT server was used (de Vries and Bonvin 2011). CPORT integrates the predictions of total six prediction tools. These comma-separated residue sites were fed along with IL-2 and IL-2R α to the HADDOCK version 2.2 web server guru level interface (De Vries et al. 2010; van Zundert et al. 2016). Default conditions were set up. Based on the docking results, the top cluster with the lowest HADDOCK score was picked. HADDOCK scores were compared to analyze the strength of protein-protein interactions. Hydrogen bonds and other intermolecular contacts were also analyzed by the PDBsum server (Laskowski 2001). Moreover, the interface residues were noticed and highlighted accordingly.

Gibbs free energy analysis of IL-2/IL-2 variants with IL-2R α

The thermodynamic properties of binding interaction between IL-2/IL-2 variants and IL-2R α were investigated by the PRODIGY web server (Xue et al. 2016) with default parameters. This server calculates the Gibbs free energy changes (ΔG). ΔG is a crucial value to understand the binding association within a biological complex and its thermodynamic feasibility (Dar et al. 2020). ΔG values less than zero indicate the energetically feasible biological complex formation.

Results

Obtaining stabilized structures of wild-type and single-point variant IL-2

The wild-type structure of IL-2 with PDB ID 1M47 (Arkin et al. 2003) was obtained from the Protein Databank resource (Burley et al. 2018). After loop modeling, IL-2 structure was obtained. MD simulation was performed on this and all other single-point variant structures.

Stability of MD simulations was assessed by analyzing the RMSD backbone. Although fluctuations in the RMSD were observed, still all systems converged toward the end of simulation (Fig. 1A). Also contrary to expectations, E61A, Y45A and E61A mutations in the IL-2 did not change the radius of gyration values in IL-2 (Fig. 1B). In fact, the mean Rg values for WT IL-2, F42A, Y45A, and E61A were found to be quite similar, with minimum fluctuations. Therefore, both the WT and mutant structures maintained their conformational compactness. Consistent with the results of radius of gyration, SASA values were found to be somewhat similar (Fig. 1C). SASA provides information about the exposed or buried status of residues. Despite the introduction of single point mutations, IL-2 conformations did not alter considerably. Therefore, we concluded that although these mutations restricted the flexibility of IL-2, the solvent exposure was not impacted. Moreover, RMSF values also conveyed the flexibility of IL-2 residues during the MD simulation (Fig. 1D).

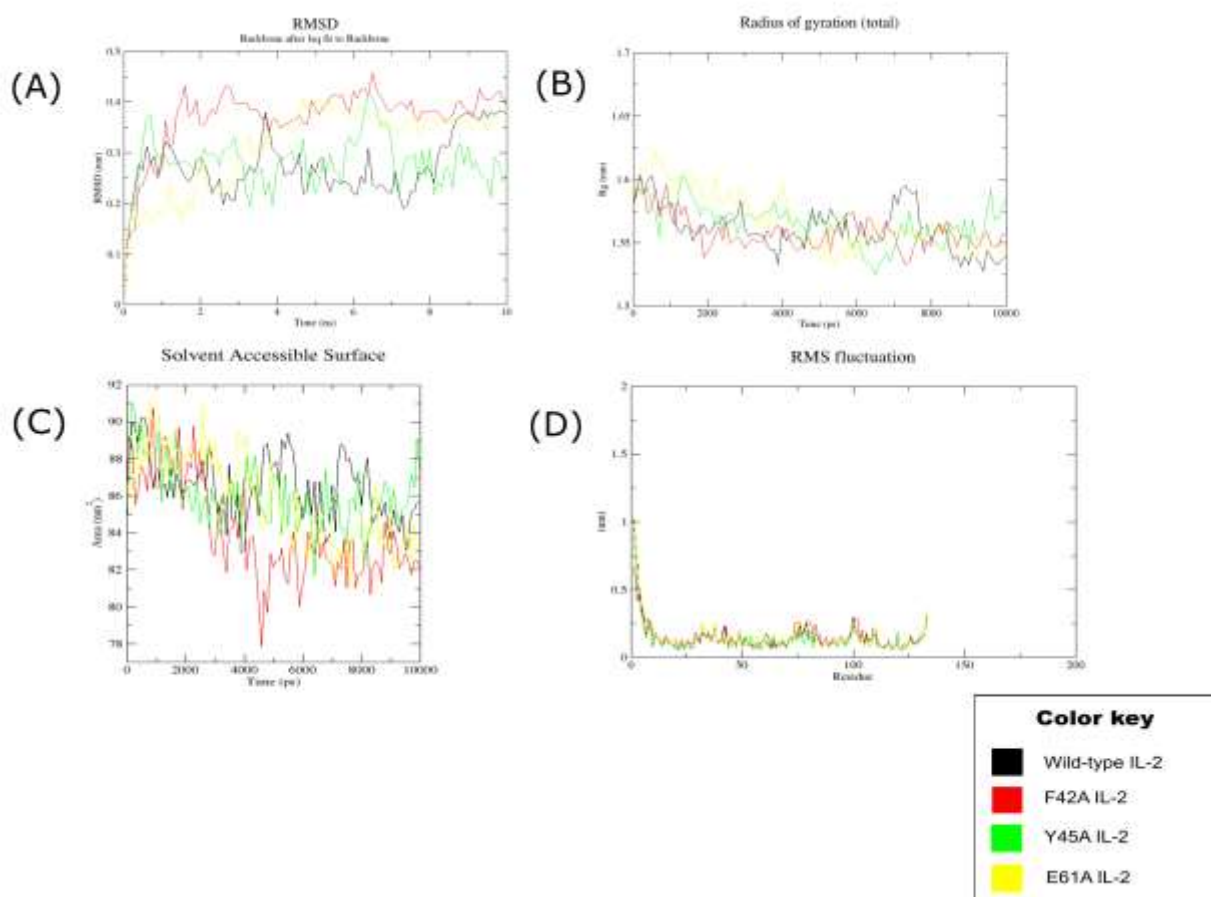


Fig. 1. MD simulation results of IL-2/IL-2 single-variant structures. (A) RMSD of backbone. As per this graph, backbone RMSD reaches upto 0.4 nm and is maintained mostly, signifying low deviations in IL-2/IL-2 variant structures. (B) Radius of gyration plot. This graph shows that IL-2/IL-2 variants maintained the compactness of

structures during simulation time. (C) SASA values showed the solvent exposure area. (D) RMSF plot. It contains certain peaks which shows flexible residues exhibiting maximum fluctuations.

After MD simulation, stabilized protein structures were obtained. Using Matchmaker option within UCSF Chimera (Pettersen et al. 2004) and keeping wild-type IL-2 structure as the reference, all the single-point variant structures were superimposed and aligned (Fig. 2).

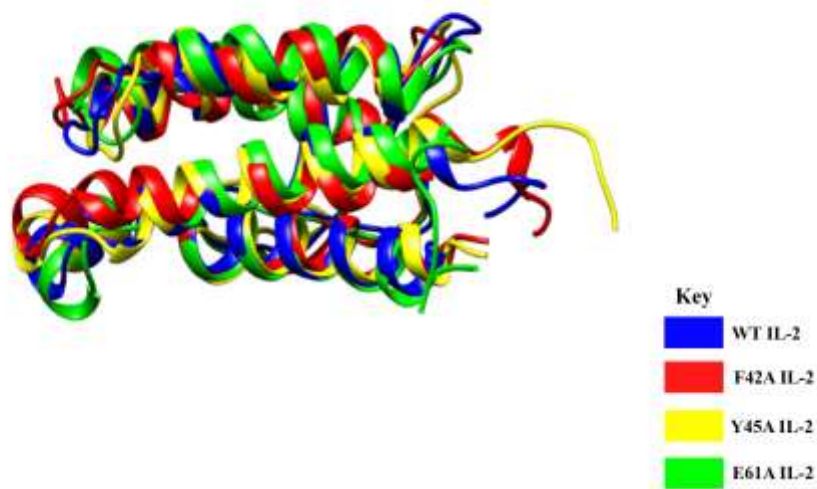


Fig. 2. Superimposition of wild-type and single-variant IL-2 structures after alignment.

Obtaining stabilized structure of IL-2R α

Due to the non-availability of complete IL-2R α crystallized structure, structural modeling was conducted. Phyre2 and SWISS-MODEL server did not generate the fully modeled structure. On the other hand, 3Dpro online tool's model quality was poor. I-TASSER and Robetta server each produced five models (Table 1). Upon structural assessments and model quality checks, Robetta model 01 was selected for molecular refinements. After molecular refinements, the top-quality structure with the best ERRAT score of 94.3231 was selected. This refined structure also had the maximum residues in the core (91.30%) and allowed (7.30%) regions.

Table 1. Evaluation results of structural models generated by different servers. One model (highlighted in bold) was selected.

Tools/server model	ERRAT score	Core region	Allowed region	General region	Disallowed region
3Dpro	49.789	83.50%	14.70%	1.40%	0.50%
I-TASSER model 01	59.6708	46.30%	39.40%	9.20%	5.00%
I-TASSER model 02	58.5062	52.30%	33.90%	10.60%	3.20%
I-TASSER model 03	63.786	52.30%	36.20%	9.60%	1.80%
I-TASSER model 04	71.1934	45.00%	39.00%	13.80%	2.30%
I-TASSER model 05	66.5289	43.10%	45.40%	9.60%	1.80%
Robetta model 01	87.7119	86.70%	11.50%	0.50%	1.40%

Robetta model 02	78.3898	84.40%	12.40%	1.80%	1.40%
Robetta model 03	83.4061	84.90%	9.20%	1.40%	4.60%
Robetta model 04	87.1795	85.30%	12.40%	0.00%	2.30%
Robetta model 05	82.0961	80.70%	15.10%	1.40%	2.80%

Molecular docking and interaction analyses

Molecular docking was performed to assess the strength of interaction between IL-2/IL-2 variants and IL-2R α . The statistics of top-ranked docked cluster along with HADDOCK scores were analyzed (**Table 2** and **Supplementary file 1**). As per results of molecular docking, the interaction strength from strongest to weakest is in the order: E61A (Strongest) > F42A > WT > Y45A (Weakest). Note that a low HADDOCK score is an indicator of better interaction potential between the docked protein chains. Interacting residues in docked protein chains were also noted and visualized accordingly (**Fig. 3**, **Fig. 4**).

Table 2. Statistical properties of the top-ranked docked clusters of IL-2 (or variants) with IL-2R α . The HADDOCK score is highlighted in bold color.

Top-cluster properties	WT	F42A	Y45A	E61A
Size of cluster	10	4	12	14
RMSD from the minimum energy structure	1.9 \pm 1.5	0.8 \pm 0.5	16.9 \pm 0.1	0.7 \pm 0.4
Van der Waals energy	-51.4 \pm 5.7	-63.0 \pm 3.0	-68.9 \pm 4.1	-56.7 \pm 7.3
Electrostatic energy	-267.5 \pm 21.9	-211.5 \pm 28.4	-142.5 \pm 23.4	-305.6 \pm 31.9
Desolvation energy	7.0 \pm 9.6	-10.4 \pm 8.2	-9.1 \pm 7.4	-15.1 \pm 5.5
Restraints violation energy	323.6 \pm 64.43	350.1 \pm 70.21	507.7 \pm 43.65	385.4 \pm 39.84
Area of Buried Surface	1880.9 \pm 147.4	1899.2 \pm 60.7	1838.4 \pm 85.2	1927.7 \pm 107.6
Z-Score	-1.3	-2.1	-1.7	-1.9
HADDOCK score	-65.5 \pm 11.6	-80.7 \pm 13.8	-55.8 \pm 3.3	-94.4 \pm 7.2

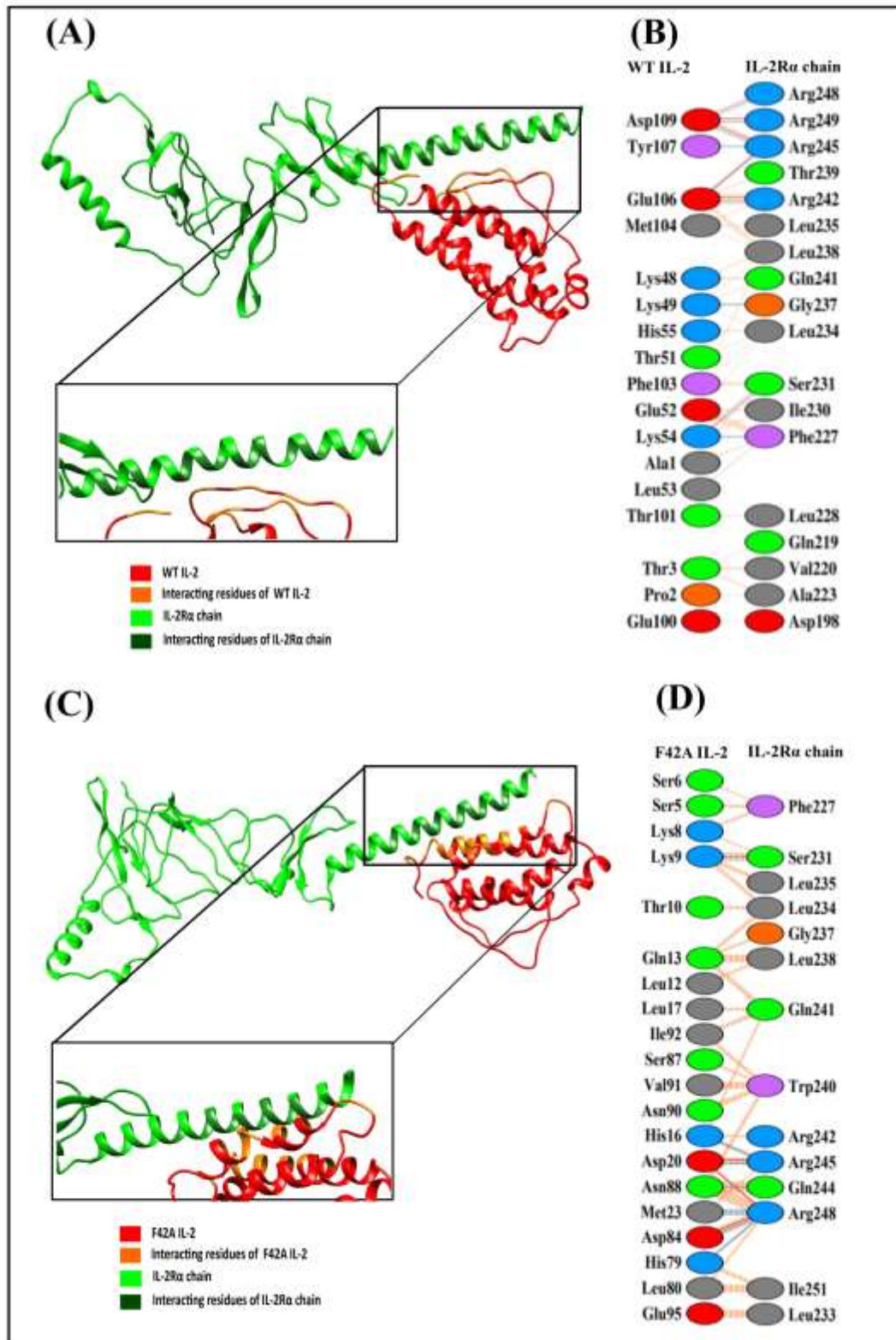


Fig. 3. Interaction analysis of WT IL-2 and F42A IL-2 with IL-2R α . (A) Docked complex of WT IL-2/IL-2R α showing some crucial interacting residues highlighted. (B) A colorful figure showing interface residues in both WT IL-2 and IL-2R α . (C) The docked complex of F42A IL-2/IL-2R α showing some crucial interacting residues highlighted. (D) A colorful figure showing interface residues in both F42A IL-2 and IL-2R α .

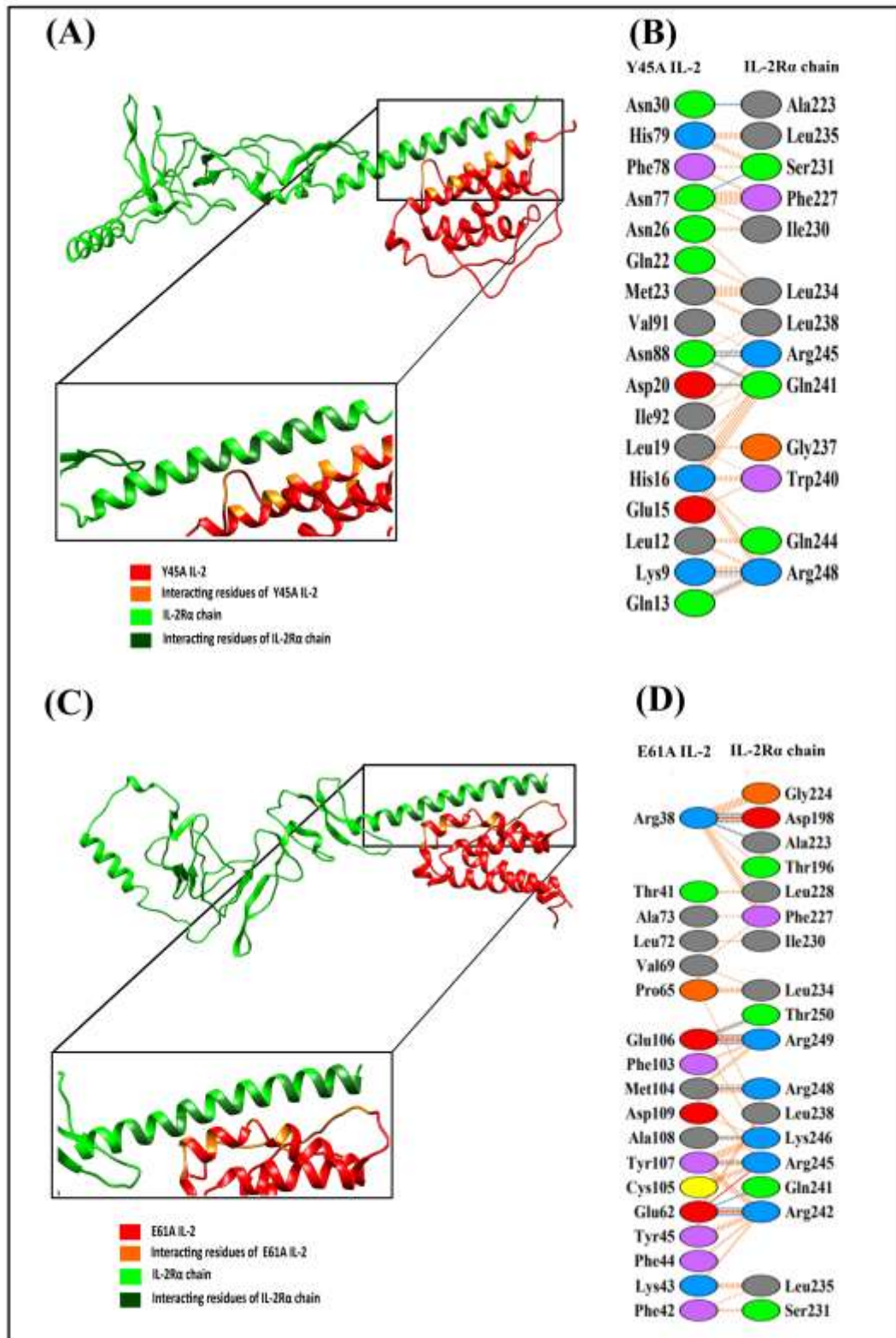


Fig. 4. Interaction analysis of Y45A IL-2 and E61A IL-2 with IL-2R α . (A) Docked complex of Y45A IL-2/IL-2R α showing some crucial interacting residues highlighted. (B) A colorful figure showing interface residues in both Y45A IL-2 and IL-2R α . (C) Docked complex of E61A IL-2/IL-2R α showing some crucial interacting residues highlighted. (D) A colorful figure showing interface residues in both E61A IL-2 and IL-2R α .

Binding affinity analysis of IL-2/IL-2 variants with IL-2R α

PRODIGY server-based free energy calculation results are described in **Table 3**. Briefly, the binding free energies of IL-2R α with IL-2/IL-2 variants were calculated to be as follows: -10.1 kcal mol⁻¹ (WT IL-2), -10.6 kcal mol⁻¹ (F42A IL-2), -12.0 kcal mol⁻¹ (Y45A IL-2), and -10.4 kcal mol⁻¹ (E61A IL-2). These results also convey the trend that mutation further stabilized the interaction of IL-2 with its cognate receptor.

Table 3. PRODIGY server results for IL-2/IL-2 variants docked complexes with IL-2 receptor.

Parameters	WT	F42A	Y45A	E61A
ΔG (kcalmol ⁻¹)	-10.1	-10.6	-12	-10.4
Kd (M) at °C	3.90E-08	1.60E-08	1.70E-09	2.20E-08
ICs charged-charged	7	7	9	10
ICs charged-polar	8	7	8	5
ICs charged-apolar	23	14	12	25
ICs polar-polar	1	6	2	1
ICs polar-apolar	9	18	21	8
ICs apolar-apolar	11	6	13	14
NIS charged	23.88	24.48	24.92	23.41
NIS apolar	39.33	36.87	37.24	39.31

Discussion

While IL-2 crystal structure was available, it had many loops. These internal missing residues were modeled by the Modeller tool (Webb and Sali 2016). Moreover, single-point mutations were manually introduced. Both the IL-2 wild type and its single-point variants were then subjected to classical MD simulation for 10 nanoseconds to acquire stabilized IL-2/IL-2 variant structures. Insights derived from MD simulation experiments were quite valuable to guide the designing of more IL-2 mutants. Our study found that mutations at sites 42, 45, and 61 did not alter the conformational structure of IL-2 considerably. Even the solvent exposure characteristic was maintained to a large extent. However, there was an indication that the flexibility of IL-2 loops may be impacted due to mutation. Our results are largely consistent with previously published studies which also confirms the validity of our approach.

By combining structural modeling and molecular refinements, a reasonably good quality protein structure of IL-2R α was obtained. Assessment by the ProSA-web server indicated that this structure lies very close to similar-sized NMR and X-ray structures. Also, stereochemical quality check by PROCHECK showed that maximum residues localized in the core and allowed regions whereas only 1.4% of modeled residues were localized in the outlier region. Also, this refined structure had a high ERRAT score of 94.3231 which supports our strategy of model selection.

Molecular docking is extensively applied in biophysics to study the potential interaction of proteins as well as other biomolecules (Guedes et al. 2014; Soler et al. 2016; Kozakov et al. 2017). To comprehend the stability and flexibility of protein chains upon docking, the guru interface of HADDOCK tool was quite helpful. HADDOCK

considers both biophysical approaches and/or biochemical data wherever applicable for docking interaction (Siddiq et al. 2016). A negative docking score is a good indicator of strong interactions between the docked protein chains. RMSD analyses also confirmed minimal structural deviations of individual protein structures upon docking. Moreover, free energy calculations by the PRODIGY server shed light on the thermodynamic feasibility of molecular interaction in nature. Altogether, a strong basis of molecular interaction was observed. Despite the introduction of single-point mutations, the IL-2 structure not only maintained its compactness but also developed stronger interactions with IL-2R α . A few crucial molecular bonding events like hydrogen bonds, and non-covalent interactions were also noticed hereby.

Unfortunately, we did not conduct specialized wet laboratory experiments to authenticate the binding association dynamics of IL-2/IL-2 single-point variants with IL-2 receptor. No doubt molecular modeling and molecular dynamics are valuable methods to study the potential interactions of proteins (Guterres and Im 2020; Nabi et al. 2022). However, these analyses are purely computational and should be verified by more biological tests. Nevertheless, our work is a valuable addition to other published research on the subject matter. Very few published studies explored the detailed amino-acid level interaction between IL-2/IL-2 variants and IL-2R α by molecular modeling methods. Altogether, our study not only increased our knowledge about IL-2 interaction with cognate receptor but also provided useful clues to design novel IL-2 proteins with desired therapeutic properties.

Conclusions

Human Interleukin-2 is a major cytokine involved in crucial immunomodulatory events inside our body. Mutations in the IL-2 gene may influence its structural flexibility and its onward interaction with IL-2R α . In the present study, we conducted comprehensive molecular modeling and simulation analyses to uncover the potential effect of some single-point mutations on the IL-2 structure. Moreover, molecular docking and free-energy binding association were conducted to comprehend the interaction of wild-type IL-2 and its single-variants with IL-2 receptor α . Our results are in conformity with previous studies that indicated no major changes in the cognate structure of IL-2. Molecular docking and interaction analyses collectively suggested that targeted mutations in IL-2 (42, 45, and 61) further stabilized the interaction with IL-2 receptor α . These results will pave the foundation for the design of novel IL-2 variants with the desired properties for immunotherapy or other purposes.

Data Availability Statement

All data generated or analyzed during this study are included in this published article [and its supplementary information files].

Competing interests

The Author(s) declare(s) that there is no conflict of interest.

Funding Statement

This research did not receive any specific grant from funding agencies in the public, commercial, or not-for-profit sectors.

References

1. Abbas AK, Trotta E, R. Simeonov D, et al (2018) Revisiting IL-2: Biology and therapeutic prospects. *Sci Immunol* 3:eaat1482
2. Arkin MR, Randal M, DeLano WL, et al (2003) Binding of small molecules to an adaptive protein--protein interface. *Proceedings of the National Academy of Sciences* 100:1603–1608

3. Artimo P, Jonnalagedda M, Arnold K, et al (2012) ExPASy: SIB bioinformatics resource portal. *Nucleic Acids Res* 40:W597--W603
4. Baek M, DiMaio F, Anishchenko I, et al (2021) Accurate prediction of protein structures and interactions using a three-track neural network. *Science* (1979) 373:871–876
5. Beig Parikhani A, Bagherzadeh K, Dehghan R, et al (2022) Human IL-2Ra subunit binding modulation of IL-2 through a decline in electrostatic interactions: A computational and experimental approach. *PLoS One* 17:e0264353
6. Berraondo P, Sanmamed MF, Ochoa MC, et al (2019) Cytokines in clinical cancer immunotherapy. *Br J Cancer* 120:6–15
7. Bird S, Zou J, Kono T, et al (2005) Characterisation and expression analysis of interleukin 2 (IL-2) and IL-21 homologues in the Japanese pufferfish, *Fugu rubripes*, following their discovery by synteny. *Immunogenetics* 56:909–923
8. Burley SK, Berman HM, Christie C, et al (2018) RCSB Protein Data Bank: Sustaining a living digital data resource that enables breakthroughs in scientific research and biomedical education. *Protein Science* 27:316–330
9. Carmenate T, Pacios A, Enamorado M, et al (2013) Human IL-2 mutein with higher antitumor efficacy than wild type IL-2. *The Journal of Immunology* 190:6230–6238
10. Cheng J, Randall AZ, Sweredoski MJ, Baldi P (2005) SCRATCH: a protein structure and structural feature prediction server. *Nucleic Acids Res* 33:W72--6. <https://doi.org/10.1093/nar/gki396>
11. Colovos C, Yeates T (1993) ERRAT: an empirical atom-based method for validating protein structures. *Protein Science* 2:1511--1519
12. Consortium U (2019) UniProt: a worldwide hub of protein knowledge. *Nucleic Acids Res* 47:D506--D515
13. Dar HA, Waheed Y, Najmi MH, et al (2020) Multiepitope subunit vaccine design against COVID-19 based on the spike protein of SARS-CoV-2: an in silico analysis. *J Immunol Res* 2020:
14. de Vries SJ, Bonvin AMJJ (2011) CPORT: A Consensus Interface Predictor and Its Performance in Prediction-Driven Docking with HADDOCK. *PLoS One* 6:e17695. <https://doi.org/10.1371/journal.pone.0017695>
15. De Vries SJ, Van Dijk M, Bonvin AMJJ (2010) The HADDOCK web server for data-driven biomolecular docking. *Nat Protoc* 5:883
16. Guedes IA, de Magalhães CS, Dardenne LE (2014) Receptor--ligand molecular docking. *Biophys Rev* 6:75–87
17. Guterres H, Im W (2020) Improving protein-ligand docking results with high-throughput molecular dynamics simulations. *J Chem Inf Model* 60:2189–2198
18. He J, Zhang R, Shao M, et al (2020) Efficacy and safety of low-dose IL-2 in the treatment of systemic lupus erythematosus: a randomised, double-blind, placebo-controlled trial. *Ann Rheum Dis* 79:141–149
19. Heaton KM, Ju G, Grimm EA (1993) Human interleukin 2 analogues that preferentially bind the intermediate-affinity interleukin 2 receptor lead to reduced secondary cytokine secretion: implications for the use of these interleukin 2 analogues in cancer immunotherapy. *Cancer Res* 53:2597–2602
20. Heaton KM, Ju G, Grimm EA (1994) Induction of lymphokine-activated killing with reduced secretion of interleukin-1 β , tumor necrosis factor- α , and interferon- γ by interleukin-2 analogs. *Ann Surg Oncol* 1:198–203
21. Heo L, Park H, Seok C (2013) GalaxyRefine: Protein structure refinement driven by side-chain repacking. *Nucleic Acids Res* 41:W384--8. <https://doi.org/10.1093/nar/gkt458>
22. Hernandez R, Pöder J, LaPorte KM, Malek TR (2022) Engineering IL-2 for immunotherapy of autoimmunity and cancer. *Nat Rev Immunol* 22:614–628
23. Kaminski GA, Friesner RA, Tirado-Rives J, Jorgensen WL (2001) Evaluation and reparametrization of the OPLS-AA force field for proteins via comparison with accurate quantum chemical calculations on peptides. *Journal of Physical Chemistry B* 105:6474–6487. <https://doi.org/10.1021/jp003919d>
24. Kelley LA, Mezulis S, Yates CM, et al (2015) The PyMol web portal for protein modeling, prediction and analysis. *Nat Protoc* 10:845–858
25. Klein C, Waldhauer I, Nicolini VG, et al (2017) Cergutuzumab amunaleukin (CEA-IL2v), a CEA-targeted IL-2 variant-based immunocytokine for combination cancer immunotherapy: Overcoming limitations of aldesleukin and conventional IL-2-based immunocytokines. *Oncoimmunology* 6:e1277306
26. Kozakov D, Hall DR, Xia B, et al (2017) The ClusPro web server for protein--protein docking. *Nat Protoc* 12:255–278

27. Krieg C, Létourneau S, Pantaleo G, Boyman O (2010) Improved IL-2 immunotherapy by selective stimulation of IL-2 receptors on lymphocytes and endothelial cells. *Proceedings of the National Academy of Sciences* 107:11906–11911
28. L Alaofi A, others (2022) IL-2 Flexible Loops Might Play a Role in IL-2 Interaction with the High-Affinity IL-2 Receptor: A Molecular Dynamics (MD) Study. *J Chem* 2022:
29. Laskowski RA (2001) PDBsum: summaries and analyses of PDB structures. *Nucleic Acids Res* 29:221–2. <https://doi.org/10.1093/NAR/29.1.221>
30. Laskowski RA, MacArthur MW, Moss DS, Thornton JM (1993) PROCHECK: a program to check the stereochemical quality of protein structures. *J Appl Crystallogr* 26:283–291
31. Lindahl E, Abraham M, Hess B, der Spoel D (2020) Gromacs 2020 Manual
32. Lotze MT, Frana LW, Sharrow SO, et al (1985) In vivo administration of purified human interleukin 2. I. Half-life and immunologic effects of the Jurkat cell line-derived interleukin 2. *J Immunol* 134:157–166
33. Mizui M, Tsokos GC (2016) Low-dose IL-2 in the treatment of lupus. *Curr Rheumatol Rep* 18:1–7
34. Nabi F, Ahmad O, Khan YA, et al (2022) Computational studies on phylogeny and drug designing using molecular simulations for COVID-19. *J Biomol Struct Dyn* 40:10753–10762
35. Pettersen EF, Goddard TD, Huang CC, et al (2004) UCSF Chimera—A Visualization System for Exploratory Research and Analysis. *J Comput Chem* 25:1605–1612. <https://doi.org/10.1002/jcc.20084>
36. Rosenberg SA, Lotze MT, Muul LM, et al (1987) A progress report on the treatment of 157 patients with advanced cancer using lymphokine-activated killer cells and interleukin-2 or high-dose interleukin-2 alone. *New England Journal of Medicine* 316:889–897
37. Rosenberg SA, Yang JC, White DE, Steinberg SM (1998) Durability of complete responses in patients with metastatic cancer treated with high-dose interleukin-2: identification of the antigens mediating response. *Ann Surg* 228:307
38. Saadoun D, Rosenzweig M, Joly F, et al (2011) Regulatory T-cell responses to low-dose interleukin-2 in HCV-induced vasculitis. *New England Journal of Medicine* 365:2067–2077
39. Siddiq A, Ahmad J, Ali A, et al (2016) Structural characterization of ANGPTL8 (betatrophin) with its interacting partner lipoprotein lipase. *Comput Biol Chem* 61:210–220
40. Soler MA, De Marco A, Fortuna S (2016) Molecular dynamics simulations and docking enable to explore the biophysical factors controlling the yields of engineered nanobodies. *Sci Rep* 6:34869
41. Stauber DJ, Debler EW, Horton PA, et al (2006) Crystal structure of the IL-2 signaling complex: paradigm for a heterotrimeric cytokine receptor. *Proceedings of the National Academy of Sciences* 103:2788–2793
42. Sun Z, Ren Z, Yang K, et al (2019) A next-generation tumor-targeting IL-2 preferentially promotes tumor-infiltrating CD8+ T-cell response and effective tumor control. *Nat Commun* 10:3874
43. Tang A, Harding F (2019) The challenges and molecular approaches surrounding interleukin-2-based therapeutics in cancer. *Cytokine X* 1:100001
44. Thanos CD, DeLano WL, Wells JA (2006) Hot-spot mimicry of a cytokine receptor by a small molecule. *Proceedings of the National Academy of Sciences* 103:15422–15427
45. Turner P (2005) XMGRACE, Version 5.1. 19. Center for Coastal and Land-Margin Research, Oregon Graduate Institute of Science and Technology, Beaverton, OR
46. van Zundert GCP, Rodrigues JPGLM, Trellet M, et al (2016) The HADDOCK2.2 Web Server: User-Friendly Integrative Modeling of Biomolecular Complexes
47. Waterhouse A, Bertoni M, Bienert S, et al (2018) SWISS-MODEL: homology modelling of protein structures and complexes. *Nucleic Acids Res* 46:W296--W303
48. Webb B, Sali A (2016) Comparative protein structure modeling using MODELLER. *Curr Protoc Bioinformatics* 54:5–6
49. Wiederstein M, Sippl MJ (2007) ProSA-web: interactive web service for the recognition of errors in three-dimensional structures of proteins. *Nucleic Acids Res* 35:W407--W410. <https://doi.org/10.1093/nar/gkm290>
50. Xue LC, Rodrigues JP, Kastiris PL, et al (2016) PRODIGY: a web server for predicting the binding affinity of protein--protein complexes. *Bioinformatics* 32:3676–3678
51. Zhang Y (2008) I-TASSER server for protein 3D structure prediction. *BMC Bioinformatics* 9:40